JET–P(98)09

MHD Stability of JET High Performance Discharges; Comparison of MHD Calculations with Experimental Observations

G T A Huysmans.

JET Joint Undertaking, Abingdon, Oxfordshire, OX14 3EA,

Preprint of a paper to be submitted for publication in the proceedings of the Workshop on Stochastic Transport (Brussels December 1997)

March 1998

1. INTRODUCTION

One of the aims of the JET, the Joint European Torus, project is to optimise the maximum fusion performance as measured by the neutron rate. At present, two different scenarios are developed at JET to achieve the high performance the so-called Hot-Ion H-mode scenario and the more recent development of the Optimised Shear scenario. Both scenarios have reached similar values of the neutron rate in Deuterium plasmas, up to $5\ 10^{17}$ neutrons/second. Both scenarios are characterised by a transport barrier, i.e., a region in the plasma where the confinement is improved. The Hot-Ion H-mode has a transport barrier at the plasma boundary just inside the separatrix, an Optimised Shear plasma exhibits a transport barrier at about mid radius. Associated with the improved confinement of the transport barriers are locally large pressure gradients (see fig.9 and 11). It is these pressure gradients which, either directly or indirectly, can drive MHD instabilities. The instabilities limit the maximum performance. In the optimised shear scenario a global MHD instability leads to a disruptive end of the discharge. In the Hot-Ion H-mode plasmas, so-called Outer Modes can occur which are localised at the plasma boundary and lead to a saturation of the plasma performance.

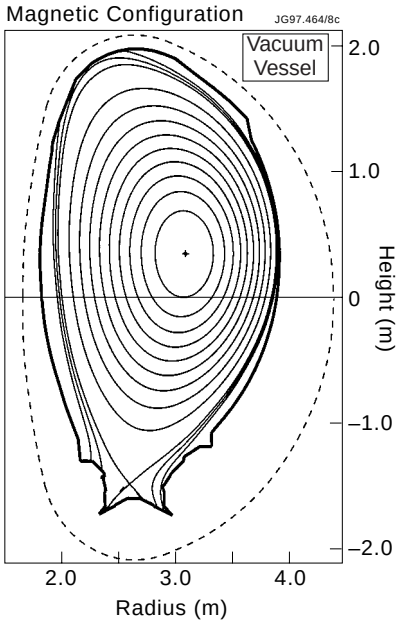

Fig. 1 The geometry of a JET high performance plasma, shown are the toroidally symmetric equilibrium flux surfaces and the limiting surfaces of the inside of the vessel. The toroidal magnetic field is 3.4-3.8 T, the current in the plasma is 3.3-4.1 MA.

In this paper, two examples of the MHD instabilities are discussed and identified by comparing the experimentally observed modes with theoretical calculations from the ideal MHD code MISHKA-1. Also, the MHD stability boundaries of the two scenarios are presented. Section 3 contains a discussion of the mode observed just before the disruption, i.e. the disruption precursor, in an Optimised Shear discharge. The Outer-Mode observed in the Hot-Ion H-mode is the subject of Section 4. In this section it is also shown how the identification of the Outer Mode has lead to a method of stabilising or delaying the onset of the mode, thereby improving the reliability of the Hot-Ion H-mode discharges.

The model that is used

2. MHD STABILITY CALCULATIONS

for the comparison with the structure of the observed modes and in the calculation of the stability boundaries is the incompressible ideal magnetohydrodynamics (MHD) model[1]. MHD is the simplest model to describe the gross macroscopic movements, waves and instabilities, of the plasma, treating the plasma as an ideally conducting fluid embedded in a magnetic field. Although the observed instabilities in the plasma are in principle non-linear phenomena, it is assumed that the spatial structure and the onset of the instabilities is well described by the linearised MHD equations.

The shape and the aspect ratio of the plasma have a strong influence on the mode structures. It is therefore important for the comparison with experiment that the correct geometry is used (see Fig.1).

In the calculation of the stability limits and the mode structures, the equilibrium is taken to be axisymmetric in the toroidal direction. The equilibrium equations :

$$\mathbf{J} \times \mathbf{B}_0 = \nabla p_0 , \quad \nabla \bullet \mathbf{B}_0 = 0 \tag{1}$$

($\mathbf{J}$ is the equilibrium current, $\mathbf{B}_0$ the equilibrium magnetic field and p_0 the plasma pressure) are solved numerically with the two-dimensional finite element code HELENA[2] which also calculates the geometric quantities of the straight field line co-ordinate system used in the stability calculations.

The linearised equations for perturbations of the velocity $\mathbf{v}_1$, the pressure p_1 and the vector potential $\mathbf{A}_1$ ($=\nabla \times \mathbf{b}_1$) , assuming a exponential time dependence $\sim e^{\lambda t}$, are :

$$\begin{aligned}
&\text{Momentum:} && \lambda \rho_0 \mathbf{v}_1 && = -\nabla p_1 + (\nabla \times \mathbf{B}_0) \times (\nabla \times \mathbf{A}_1) - \mathbf{B}_0 \times (\nabla \times \nabla \times \mathbf{A}_1) \\
&\text{Energy:} && \lambda p_1 && = -\mathbf{v}_1 \bullet \nabla p_0 - \gamma p_0 \nabla \bullet \mathbf{v}_1 \\
&\text{Faraday Law:} && \lambda \mathbf{A}_1 && = -\mathbf{B}_0 \times \mathbf{v}_1
\end{aligned} \tag{2}$$

With the constraints of incompressible ideal MHD, i.e.

$$\mathbf{A}_1 \bullet \mathbf{B}_0 = 0, \qquad \mathbf{v}_1 \bullet \mathbf{B}_0 = 0, \qquad \nabla \bullet \mathbf{v}_1 = 0 \tag{3}$$

the set of Equations (2,3) can be reduced to two equations for the components of the perturbed velocity in the direction perpendicular and parallel to the flux surfaces. Due to the symmetry of the equilibrium, the dependence of the perturbations on the toroidal angle can be described by one toroidal mode number, n. The recently developed MISHKA-1 code[3] is used to solve the two equations. In the MISHKA-1 code the poloidal dependence of the two variables is described by a Fourier series, the radial dependence by cubic and quadratic finite elements. A Galerkin method is used to form a generalised matrix eigenvalue problem of the form $\boldsymbol{A}\,\mathbf{x} = \lambda\, \boldsymbol{B}\,\mathbf{x}$ which is solved with inverse vector iteration[4].

3. OPTIMISED SHEAR DISCHARGES

The good performance of the Optimised Shear (OS) discharges[5] is due to a characteristic transport barrier at about mid radius of the plasma. The occurrence of the transport barrier is related to the shape of the q-profile. A typical q-profile in the JET optimised shear discharges has a low shear in the plasma centre with a value of q on axis between 1.5 and 2. These q-profiles are obtained by early heating of the plasma during a long ramp of the plasma current. Fig.2 shows the time evolution of one of the best JET OS discharges in deuterium. With the start of the beam heating the transport barrier forms, resulting in extremely high central ion temperatures and a peaked pressure profile.

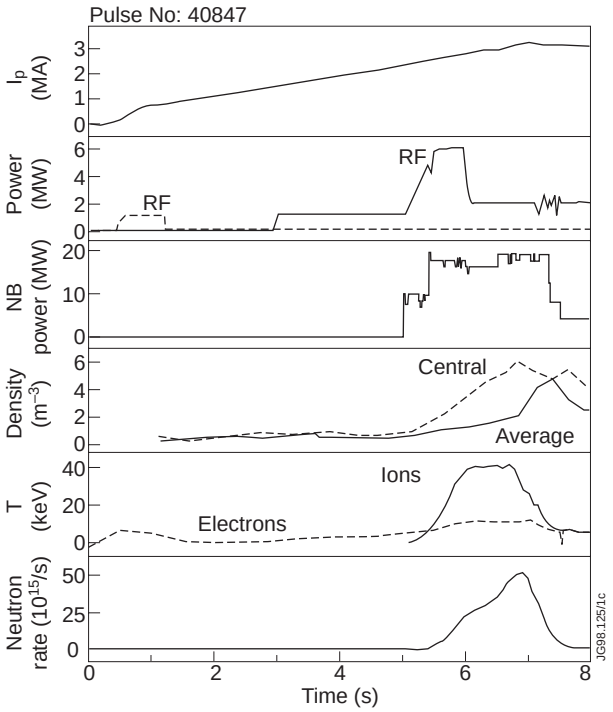

Fig.2 Time traces of the plasma current, the heating power, the density, the electron and ion temperature on axis and the neutron rate for discharge 40847.

Disruptions (a sudden termination of a discharge within one millisecond due to an MHD instability) are common in the OS discharges. The disruptions can be avoided by careful programming of the heating power (see section on the MHD stability limits). In this case, the reduction in the RF power and the neutral beam power at t=5.8 seconds was found to be necessary to avoid a disruption. This however also limits maximum fusion performance.

Tomographic reconstruction of the disruption precursor

Some of the disruptions show a clear precursor, i.e. an instability growing to large amplitude just before the disruption occurs. Fig.3 shows an example of a discharge (#39430) in which the heating power was not stepped down and a disruption occurs at t=6.8s. The disruption occurs at a relatively low value of the normalised beta of β_N =1.6 ($\beta_N = \mu_0 <p> a [m] /(B [T] I [MA]$, <p> is the volume averaged pressure, a the minor radius, B the toroidal field and I the plasma current). In another type of discharges, which aim at high β_N, without a strong transport barrier and large pressure gradients, normalised beta values just below 4 can be obtained[6].

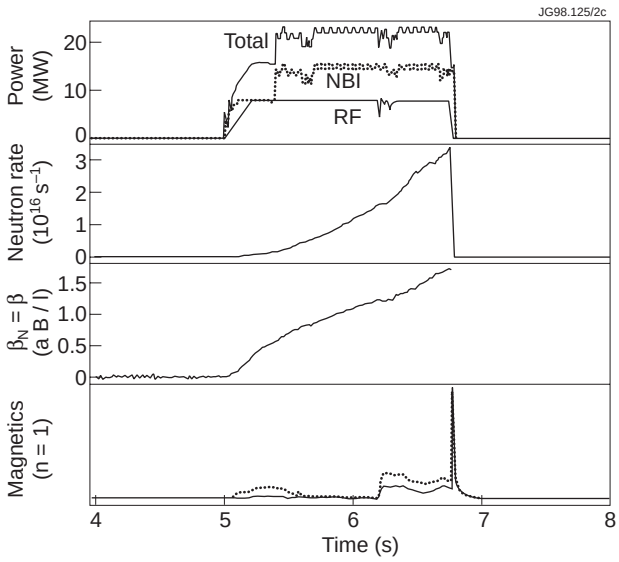

Fig.3 The heating power, neutron rate, the normalised beta and n=1 magnetics as a function of time for discharge 39430.

The precursor to the disruption is clearly seen in the fast diagnostics, the magnetic pick-up coils, the electron temperature (ECE) and the SXR cameras. Fig. 4 shows the time evolution of one channel of a SXR camera which views through the plasma centre. The mode grows within 1 millisecond to its maximum amplitude while it slows down in frequency from 30kHz, the rotation frequency of the plasma centre, down to 0 kHz at which point the plasma disrupts. The toroidal mode number of the precursor is n=1 as determined from an array of 10 magnetic pickup coils located at different toroidal angles.

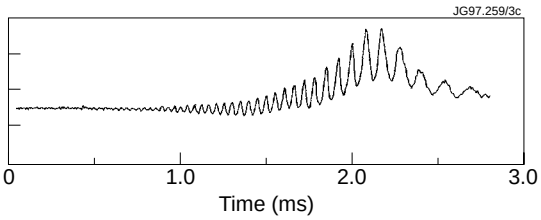

Fig.4 The precursor of the disruption in discharge #39430 as seen in a central SXR channel.

The SXR diagnostic at JET[7] consists of 6 cameras distributed at different poloidal angles on the outboard side of the plasma. In total there are 176 channels viewing the plasma. The large number of channels allows the tomographic reconstruction of SXR emission profile in two dimensions. With the six SXR cameras three poloidal harmonics of the SXR emission can in principle be resolved. For the tomographic reconstruction of the precursor of Fig.4 the harmonics m=0, 1 and 2 are used. The radial dependence of the emission profile is described by 8 cubic B-splines.

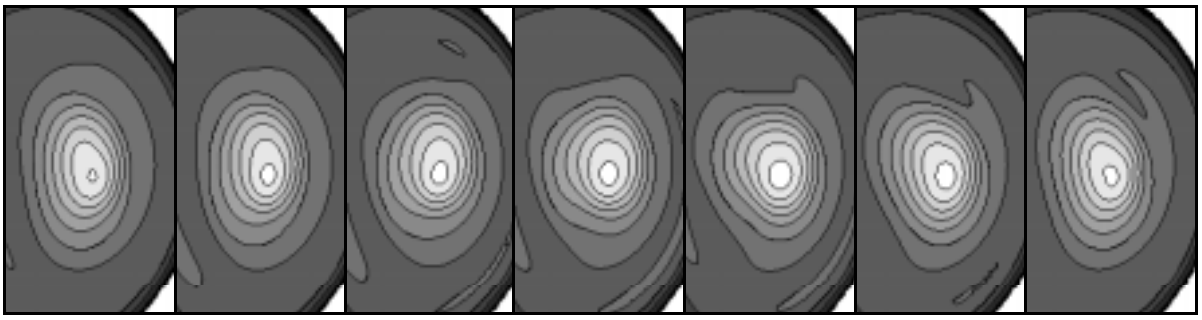

Fig.5 The perturbed SXR emission profiles for 8 time slices of one period of the disruption precursor. The time difference between each frame is 8 μs.

The results of the tomographic inversion for eight time slices in one period of the oscillation of fig.4 (around t=2.0 ms) are shown in Fig.5. The figure shows contour plots of the SXR emission in the central part of the poloidal plane. The slices are 8 μs apart. The plasma is seen to move in a combination of an m=1 rotation of the central part and an m=2 deformation which changes the elongation of the emission contours.

Comparison of the Observed Mode Structure with MHD Calculations

The theoretical mode structure can be found by analysing the stability of the equilibrium in discharge #39430 just before the disruption. The equilibrium is obtained from a reconstruction with the EFIT code[8] which fits the equilibrium to the measurements of ~40 magnetic pickup coils. The pressure profile is obtained from the measurements of the density, and the electron

and ion temperature profiles. The MISHKA-1 code is used for the MHD stability calculations. The equilibrium just before the disruption is calculated to be unstable to a global pressure driven n=1 kink mode. The spatial structure of the instability is shown in fig.6. The mode extends over the whole plasma radius and has a dominant m=2 component with m=1 and higher m harmonics as side bands.

To compare the calculated mode structure with the structure obtained from the tomographic inversion, the calculated displacement of the flux surfaces has to be multiplied with the gradient of the equilibrium SXR emission profile. This equilibrium profile is obtained by tomographic inversion of the time averaged SXR signals. Due to the extreme peakedness of the equilibrium profile, only the perturbation in the plasma centre remains visible. In Fig. 7a and 7b the perturbations of the SXR emissivity contours from the calculated mode structure and from the tomographic inversion are compared. Good agreement is found. However due to the peaking of the SXR emission profile only information of the m=1 and m=2 harmonics can be obtained. The good agreement indicates that the disruption as observed in the Optimised Shear discharges is due to a global pressure driven mode exceeding the ideal MHD stability boundary.

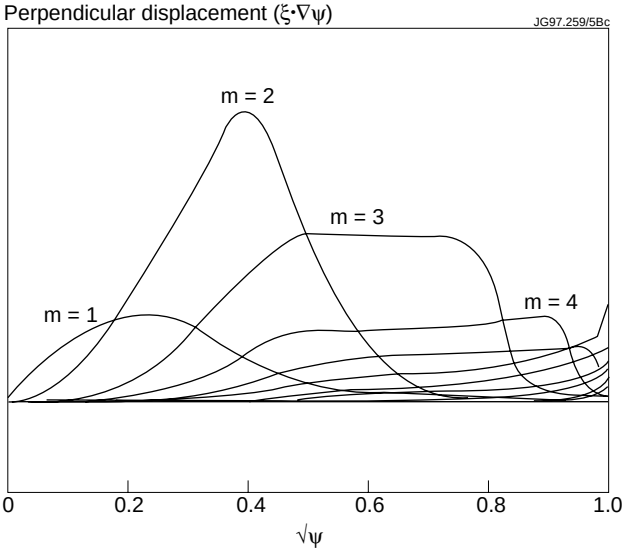

Fig.6 The poloidal harmonics of the displacement perpendicular to the flux surfaces as a function of the minor radius of the n=1 mode found unstable in discharge 39430 at the time of the disruption precursor.

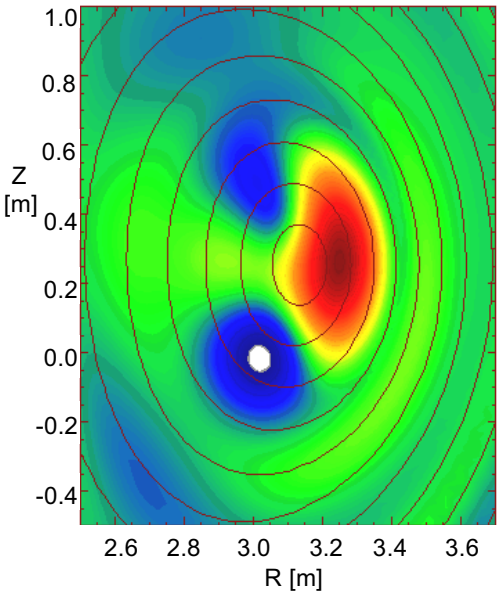

Fig.7a The difference between two time slices of the SXR tomographic reconstruction of the disruption precursor in #39430. The closed curves are the equilibrium flux surfaces.

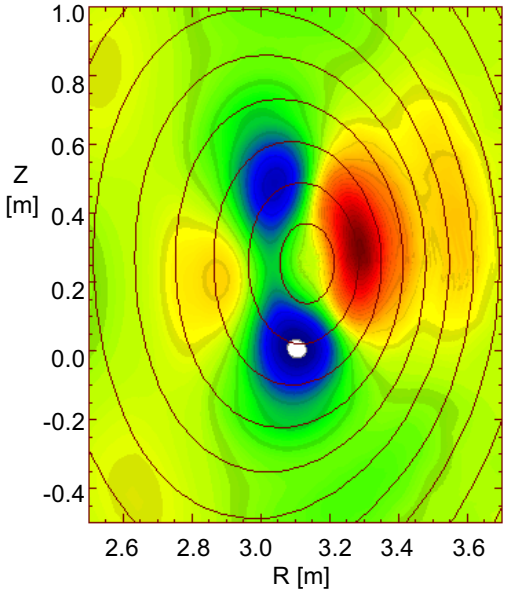

Fig.7b The simulated perturbation of the SXR emission based on the n=1 mode in fig.6.

MHD Stability Limits

With the identification of the mode that leads to the disruption in the optimised shear discharges, the relevant MHD stability limits due to this mode can be analysed. The time evolution of the calculated MHD stability limit in discharge #40847 (see fig.1) is plotted in fig.8a. The limit in the normalised beta is very low early, close to 1, and then increases above 2 at t = 7.0s. The reason for the evolution of the stability limit in time is the changing shape of the pressure profile (see Fig.9). As the transport barrier moves outward in time the peaking factor of the pressure

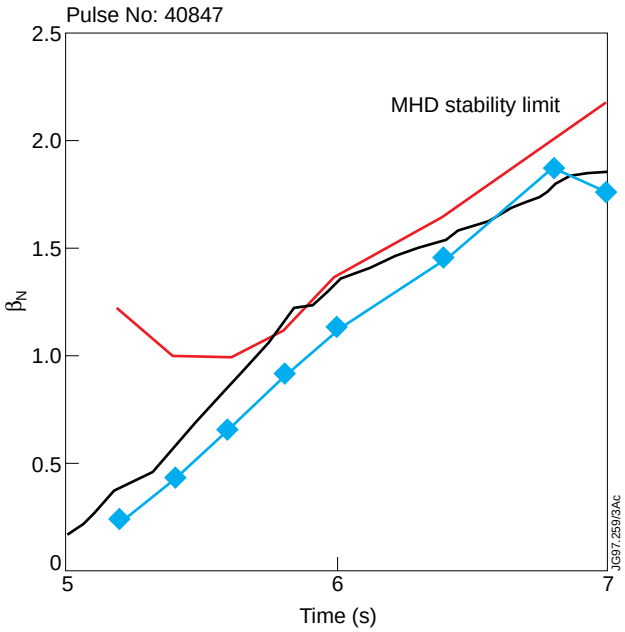

Fig.8a The MHD stability limit due to the n=1 pressure driven kink mode as a function of time for discharge #40847 (see Fig.2). Included is the time evolution of the discharge.

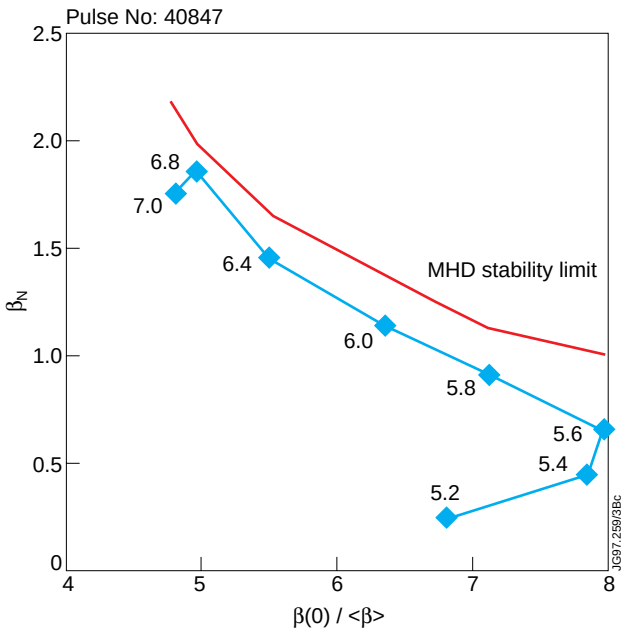

Fig.8b The MHD stability limit as a function of the peaking factor of the pressure profile.

profiles goes down such that the pressure on axis is almost constant. Fig. 8b shows the same stability limits now as a function of the peaking factor of the pressure profile. Included in Fig.8 is the experimental value of the normalised beta as a function of time. It appears that the plasma is very close to MHD stability limit for most of the main heating phase. The reduction in the heating power at t=5.8, (see fig.2), was found to be necessary in order to avoid a disruption occurring at this time, consistent with the calculated stability limits. With the knowledge of the MHD stability limits and

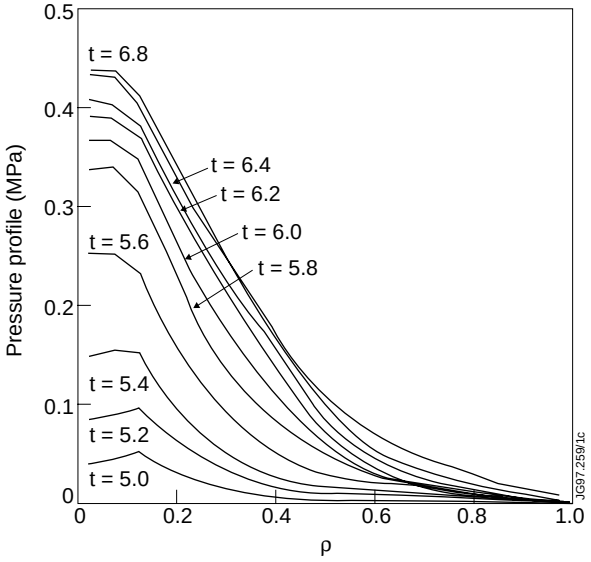

Fig.9 The evolution of the pressure profile in discharge #40847 (see fig.2).

careful programming of the heating power, making sure not to overheat the discharge in the early stages when the pressure profile is extremely peaked, the disruptions can be avoided.

4. THE OUTER MODE IN HOT-ION H-MODE DISCHARGES

In the more conventional hot-ion H-mode scenario[9], a low density plasma is heated by strong neutral beam heating. The low density ensures a good penetration of the beams into the plasma centre and a low equipartion rate between the ions and electrons. As a consequence the ions are much hotter than the electrons. At the plasma boundary a transport barrier forms, the H-mode, with a typical width of 3-4 cm. In this region large pressure gradients develop. The Hot-Ion H-mode is a transient regime where the good performance phase ends with the occurrence of an MHD instability. In the best Hot-Ion discharges, the MHD activity typically starts 1.2 - 1.5 seconds after the start of the beam heating. The MHD activity is due to either a sawtooth, a giant ELM (Edge Localised Mode) or an Outer Mode. The three modes occur roughly in equal proportion. The sawtooth is a fast relaxation (~100 μs) of the pressure in the core of the plasma and is not directly related to the transport barrier. The poloidal and toroidal mode number of the instability is m = n = 1. The giant ELM is an instability of the plasma edge which causes a loss of about 5% of the plasma energy in a very short time (<200 μs). The Outer Mode is a more benign mode located at the plasma boundary where it can exist for up to several hundred milliseconds. The Outer Mode is associated a saturation of the stored energy and the neutron rate. Fig.10 shows the time traces of the Hot-Ion H-mode discharge 38675, where an Outer Mode causes a degradation in the plasma performance. In this case the plasma recovers after the Outer Mode disappears with the occurrence of a small ELM. In most cases the Outer Mode leads to a giant ELM from which the plasma does not recover. Experimentally the Outer Mode is observed in Soft X-ray (SXR) data, the fast Electron Cyclotron Emission (ECE) data, the reflectometer data and the magnetics (Mirnov coils). The toroidal mode number is usually n=1 but higher n (2, 3 and 4) have also been observed. The frequency of the mode corresponds to the plasma rotation frequency near the plasma edge. For an n=1 mode the frequency is typically 10 kHz. The outer mode is localised in the outer 10% of the plasma (hence its name).

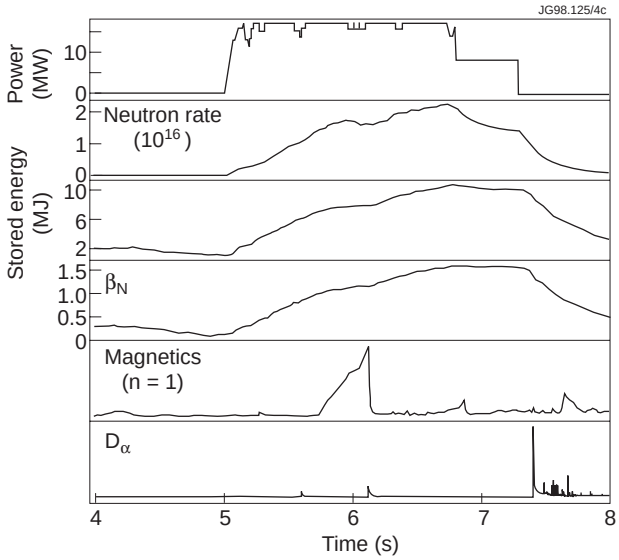

Fig. 10 The neutral beam heating power, the neutron rate, the stored energy, the normalised beta, the n=1 magnetics signal and the D_α radiation for discharge 38675, showing the influence of the Outer Mode which starts at t=12.6s and ends at 13.1s.

Comparison of the Observed Mode Structure with MHD Calculations

The pressure profile during the high performance phase of the hot-ion H-mode is characterised by large gradients at the plasma boundary. These pressure gradients drive a bootstrap current, locally increasing the current density close to the plasma boundary (see fig.11). Both the pressure gradient and the current density at the edge can drive MHD instabilities unstable. The pressure gradient can drive ballooning modes (with a high toroidal mode number and localised

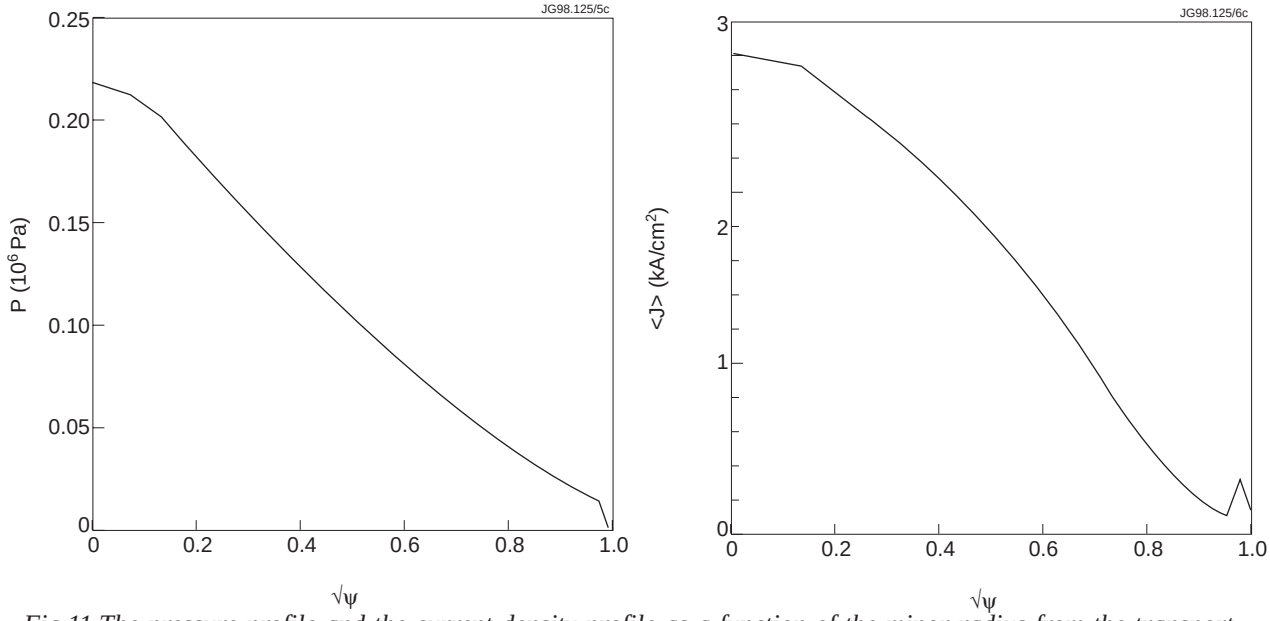

Fig.11 The pressure profile and the current density profile as a function of the minor radius from the transport simulation of discharge #38675 at the time when the outer mode is present, t=13.0s.

on the outboard side of the plasma). The current density close to the boundary can drive the low-n external kink mode unstable. Analysis of the MHD stability of the equilibrium profiles of hot-ion H-mode discharges shows that at the time the Outer Mode occurs, the plasma exceeds the n=1 external kink stability limit.

Fig. 12 shows the displacement of the flux surfaces due to the n=1 kink mode as a function of the minor radius. The localisation of the external kink mode agrees well with that of the Outer Mode. Fig. 13a shows a contour plot of the displacement in the poloidal plane. The poloidal structure of the mode is characterised by cells with a large poloidal extent on the Outboard side and much smaller cells close to the x-point. Fig. 13b shows a n=10

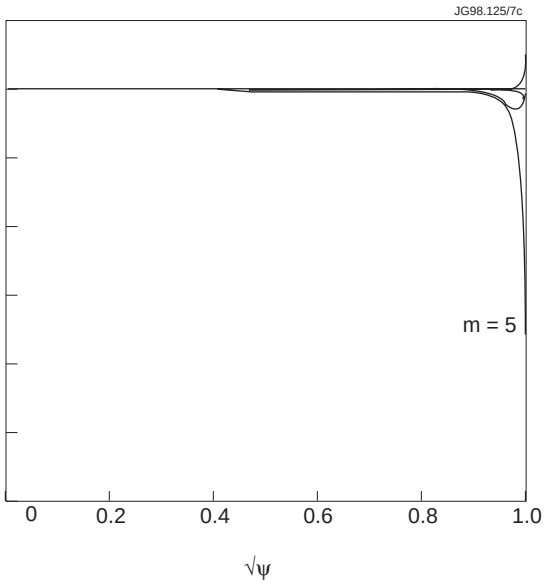

Fig. 12 The mode structure of the n=1 kink mode, the displacement of the plasma as a function of the minor radius, The mode is found unstable at the time of the Outer Mode.

ballooning mode for comparison. This n=10 ballooning mode is not normally unstable. Here it has been forced unstable by artificially increasing the edge pressure gradient. The same mode structures of the two modes are plotted in a three dimensional representation in Fig.14. Fig.14a shows a flux surface just inside the separatrix perturbed by the n=1 kink mode. The largest amplitude of the mode is close to the x-point.

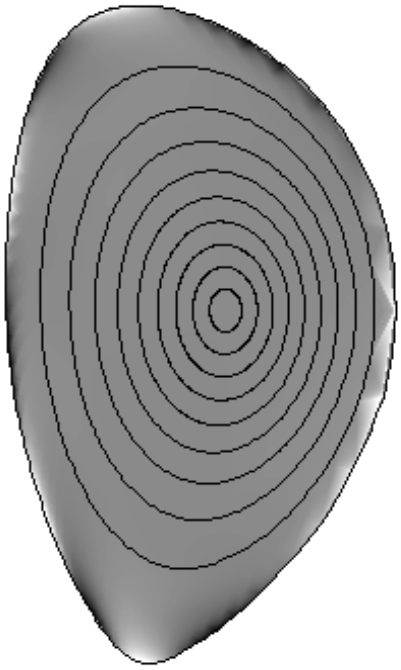

Fig. 13a Contour plot of the displacement perpendicular to the equilibrium flux surfaces due to a n=1 external kink mode (see fig. 12).

Fig.13b The displacement due to an n=10 ballooning mode. Red and Blue represent the minima and maxima of the displacement.

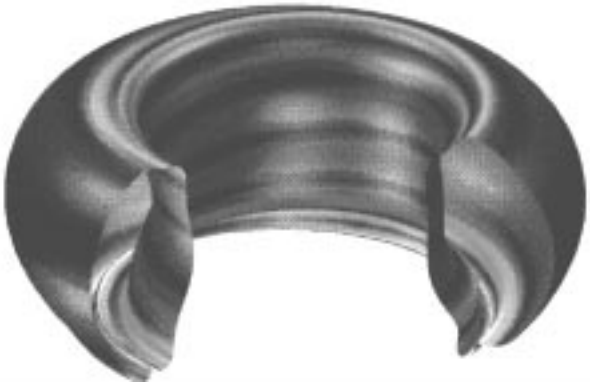

Fig14a A flux surface (ψ=0.99) perturbed by an n=1 kink mode. The amplitude of the perturbation is colour coded red is the largest amplitude black the smallest.

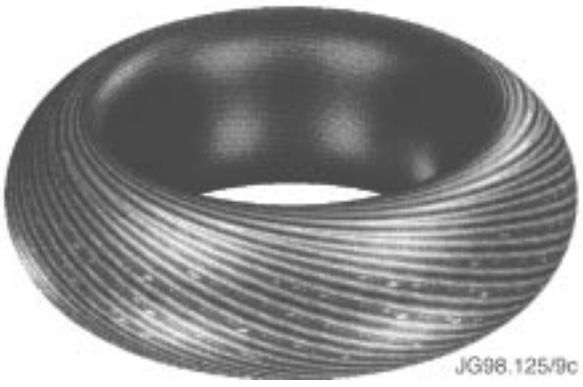

Fig. 14b The displacement of an n=10 ballooning mode (note that in this figure the flux surface is the equilibrium non-perturbed surface).

From the n=1 kink stability limits and the localisation of the kink mode it appears likely that the Outer Mode observed in the Hot-Ion H-mode discharges is a kink mode. For a more detailed identification of the Outer Mode[10], the SXR data is compared to predictions of the data based on the mode structure of the n=1 kink mode. Tomographic reconstruction of the SXR

data, as was used in the case of the disruption precursor, is extremely difficult due to the localisation of the Outer Mode and the relatively high poloidal mode number. Instead, the measured SXR data of the individual channels is compared with predictions of the SXR data based on the calculated mode structure. To calculate the predictions of the SXR signals due to the external kink mode, the kink mode displacements (see Fig. 12, 13a) are added to the equilibrium flux surfaces. This yields perturbed flux surfaces with an n=1 perturbation in the toroidal direction (see Fig.14a). It is assumed that a given SXR emissivity profile 'moves' with the perturbed flux surfaces, allowing the line integrals over the lines of sight of the SXR cameras to be calculated. Assuming that the perturbed plasma rotates toroidally with a fixed frequency (the frequency of the outer mode), the values of the line integrals at different toroidal angles can be translated into a time dependent signal. Thus, the external kink mode is assumed to be saturated at a fixed amplitude in time and the time variation comes from the toroidal rotation of the n=1 structure.

The results are shown in fig.15 where the relative phase of the SXR data is compared with the predictions for 9 SXR channels which show the largest amplitude. Excellent agreement is found. The sharp phase change of 180° between the two adjacent channels E33 and E31 observed in the SXR data is very well reproduced in the calculated phases. This phase change is due to the poloidally localised structure of the mode close to the x-point. Both channels E31 and

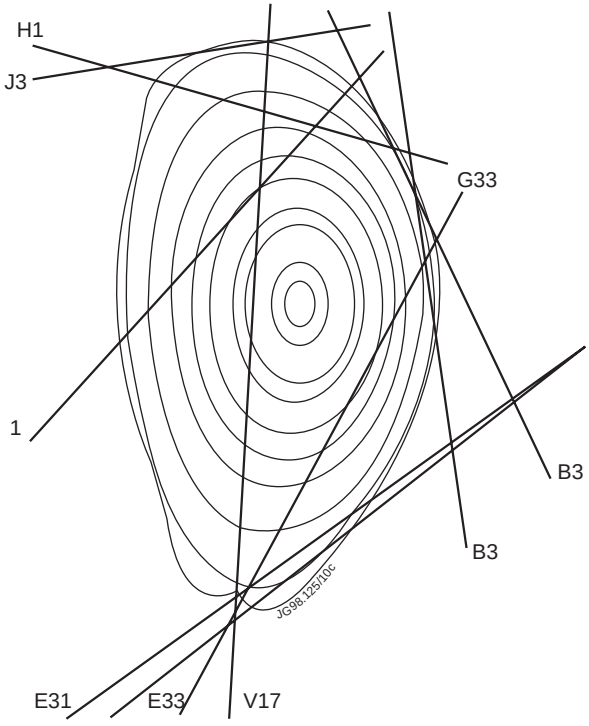

Fig.15a The channels used for the comparison. Also shown are the perturbed flux surfaces.

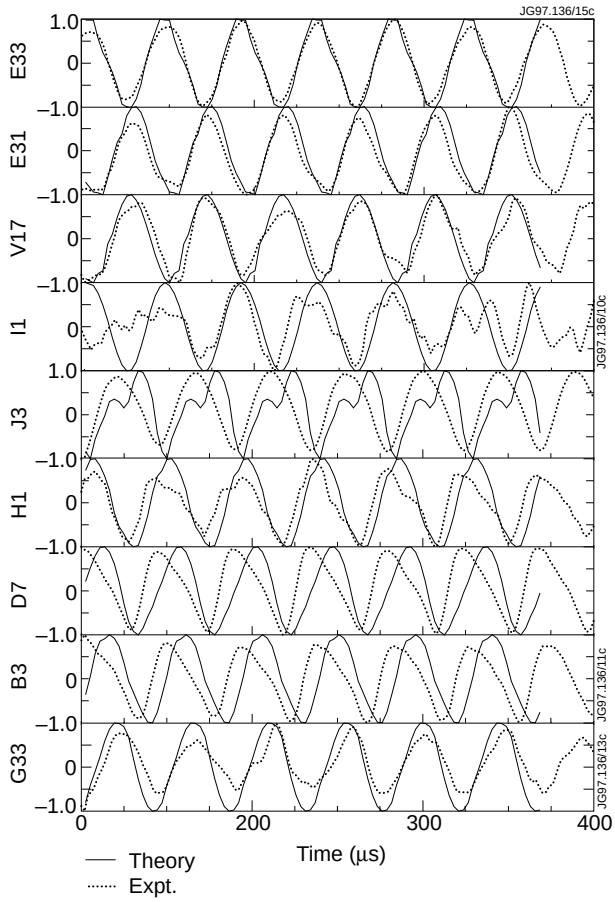

Fig. 15b Comparison of the phase of the SXR channels with the prediction based on the n=1 external kink mode.

E33 pass close to the x-point but at opposite phases of the n=1 kink perturbation. The phase of the channels on the top of the plasma and on the outboard side are also well reproduced. This yields a strong confirmation that the Outer Mode has been correctly identified as an external kink mode.

Comparison of the absolute amplitude of the SXR channels with the model, give an amplitude of movement of the flux surfaces due to the n=1 kink mode of about 1 cm on the outboard side and ~10 cm close to the x-point.

With the identification of the Outer Mode as an external kink mode it has become clear that the Outer Mode, like the external kink mode, is driven unstable by the current density close the plasma boundary in a the layer of 5-10cm from the boundary inwards. Reducing the edge current density by ramping down the total plasma current should therefore have a stabilising effect on the Outer Mode. This was confirmed by experiments. Starting a moderate ramp down of the plasma current of about 200kA/s just before the Outer Mode is expected to become unstable, successfully stabilised or delayed the onset of the Outer Mode. This is illustrated in Fig.16 which compares two discharges, one with (#40115) and one without (#40116) a current ramp. Without the current ramp an Outer Mode starts at t=12.9s which deteriorates the plasma performance. Starting a current ramp down at t=12.6 s successfully stabilises the Outer Mode until a giant ELM ends the good performance at t=13.4s.

The evolution of the two discharges with respect to the stability limits due the external kink mode and due to ballooning modes is shown in Fig. 16b as a function of the edge current

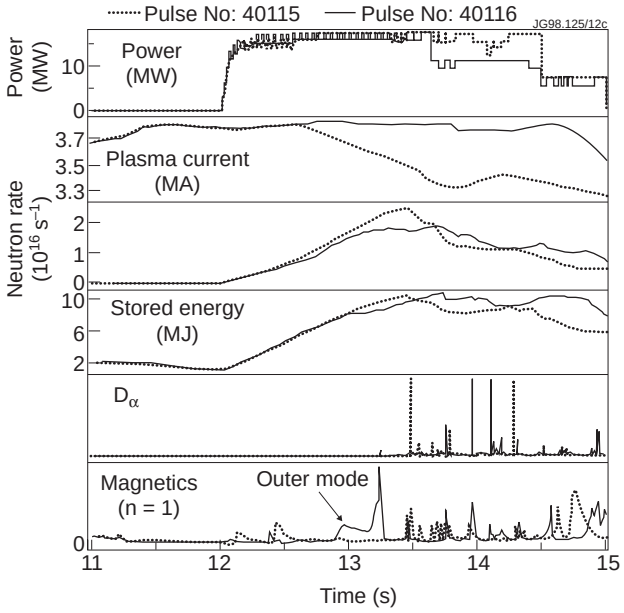

Fig. 16a Comparison of the time traces of two discharges with and without a current ramp down, showing the stabilising effect of the current ramp-down the Outer Mode.

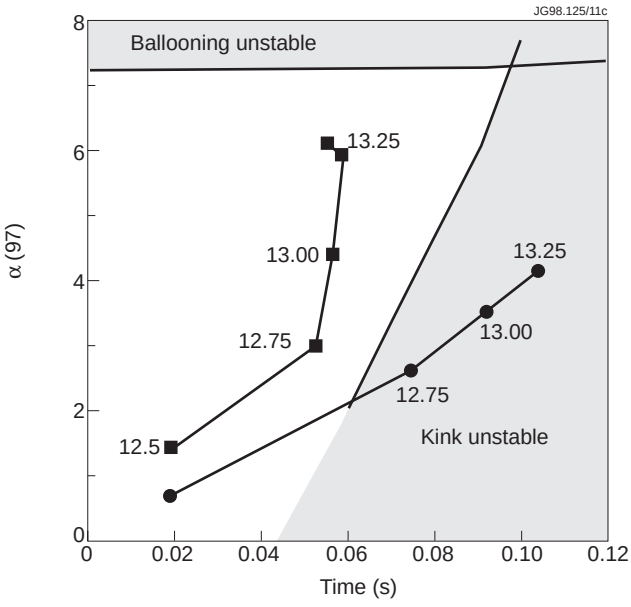

Fig. 16b The edge stability diagram for the n=1 kink mode and ballooning modes as a function of the edge current density and the normalised edge pressure gradient. Included are the time evolution of the two discharges of Fig. 16a.

density and the normalised edge pressure gradient. (α is defined as $\alpha=-2(q^2R_0/aB_0^2)dp/ds$, where p is the pressure, q is the local value of the safety factor, $s = \sqrt{\psi}$, a the minor radius, R_0 the major radius and B_0 the vacuum magnetic field in the geometric centre.) The data of the edge pressure gradient and current density is obtained from a transport simulation of the two discharges. The discharge without the current ramp crosses the kink stability boundary consistent with the occurrence of the Outer Mode. By ramping down the current, the kink stability boundary is avoided and no Outer Mode occurs. One disadvantage of ramping down the current is the increase in q which increases the normalised pressure gradient so that it gets closer to the ballooning stability limit. This may be the reason for the observation that the giant ELM occurs earlier in the discharges with a current ramp[11]

The addition of a current ramp-down has lead to an improved reliability and performance and is now a standard ingredient in the Hot-Ion H-mode scenario.

5. CONCLUSIONS

In JET, high fusion performance has been achieved in two scenarios, the Hot-Ion H-mode and the Optimised Shear scenario. The large pressure gradients associated with the transport barriers in the two scenarios lead to MHD instabilities at relatively low values of the normalised beta, limiting the fusion performance.

In the two examples presented, the disruption precursor in the Optimised Shear scenario and the Outer Mode in the Hot-Ion H-mode scenario, the ideal MHD model provides a good description of both the spatial structure of the modes and the MHD stability boundaries. Identification of the observed instabilities (the disruption precursor as a global n=1 pressure driven kink mode and the Outer Mode as an external kink mode driven by the edge current) has lead to an improved understanding and to some control/avoidance of the instabilities. This has contributed to improved reliability and performance.

ACKNOWLEDGEMENT

The contributions of T. Hender, B. Alper, V.V. Parail, G. Cottrell and Y. Baranov are gratefully acknowledged.

REFERENCES

1. J.P. Freidberg, *Ideal Magnetohydrodynamics*, Plenum Press, New York, (1987).
2. G.T.A. Huysmans, J.P. Goedbloed, and W.O.K. Kerner, *Isoparametric Bicubic Hermite Elements for the solution of the Grad-Shafranov Equation*, CP90 Conf. on Comp. Physics Proc., World Scientific Publ. Co. 1991, p.371
3. A.B. Mikhailovskii, G.T.A. Huysmans, W.O.K. Kerner, and S.E. Sharapov, *Optimisation of Computational MHD Normal Mode Analysis for Tokamaks*, Plasma Physics Reports, Vol. 24 No.10 p. 844 (1997)

4. W. Kerner, *Large Complex Eigenvalue Problems*, Journal Comp. Physics, Vol. 85, no.1 (1989).
5. F.X. Soldner and the JET team, *Shear Optimisation experiments with current profile control on JET*, Plasma Phys. Control. Fusion 39 (1997) B353.
6. G.T.A. Huysmans, G. Cordey, C. Gormezano, A.C.C. Sips and B.J.D. Tubbing, *v* Dependence of the Beta Limit in JET*, 24th EPS Conference on Controlled Fusion and Plasma Physics, Berchtesgaden, Vol. 21A, p.1857 (1997).
7. B. Alper et al, Rev. Sci. Instr. **68**, 778 (1977).
K. Blackler and A. W. Edwards, IEEE Trans. Nucl. Sci. **41**, 111 (1994)
8. LAO L., et al. , Nucl. Fusion **30** (1990), p.1035.
9. The JET team, Plasma Phys. Control. Fusion **37** (1995), p. A359.
T.T.C. Jones and the JET team, Phys. Plasmas **4**, No. 5 (1997), p.1725.
10. G.T.A. Huysmans, T. Hender and B. Alper, *Identification of external kink modes in JET*, Nuclear Fusion, Vol. 38 no.2 (1998).
11. M.F.F. Nave et al., *Discharge Optimisation and the control of MHD modes*, 24th EPS Conference on Controlled Fusion and Plasma Physics, Berchtesgaden, Vol. 21A, p.1 (1997).